Phonon mode behaviours of $PbTiO_3$ thin films deposited on Pt/Si substrates

2000 J. Phys.: Condens. Matter 12 399

(http://iopscience.iop.org/0953-8984/12/4/304)

J. Phys.: Condens. Matter **12** (2000) 399–414. Printed in the UK PII: S0953-8984(00)02917-9

Phonon mode behaviours of $PbTiO_3$ thin films deposited on Pt/Si substrates

D S Fu†‡, H Iwazaki†, H Suzuki§ and K Ishikawa†

† Research Institute of Electronics, Shizuoka University, Johoku 3-5-1, Hamamatsu 432-8011, Japan

‡ Department of Physics, Zhongshan University, Guangzhou 510275, People's Republic of China

§ Faculty of Engineering, Shizuoka University, Johoku 3-5-1, Hamamatsu 432-8561, Japan

Received 19 March 1999, in final form 9 November 1999

Abstract. Phonon mode behaviours are investigated as a function of temperature from room temperature to 534 °C for $PbTiO_3$ thin films deposited by the sol–gel method on Pt/Si substrates. Intense Raman scattering is observed at all temperatures. The spectra are analysed with a classical oscillator model to estimate the frequencies and damping factors of soft E(1TO) and A_1(1TO) modes, and are compared with those of bulk single crystals. The spectrum consists of a remarkable central-mode-type scattering at all temperatures. All transverse optical modes are observed and proved to have a shift from their position in bulk single crystal. The soft E(1TO) and A_1(1TO) modes do not appear to soften further on heating toward the ferroelectric–paraelectric transition. Their damping factors are larger, and do not diverge near the phase transition, in contrast to the findings of previous studies on bulk single crystal. The static dielectric constants along principal axes are calculated using the Lyddane–Sachs–Teller relationship as a function of temperature and are compared with those of the bulk single crystals. The Curie–Weiss constant derived from the temperature dependence of the dielectric constant along the *c*-axis has a value of 3.27×10^5 °C. The ferroelectric phase is expected to be stable up to a temperature as high as 577 °C for these films. A modified Devonshire thermodynamic theory is shown to be plausible for the explanation for the shifts in Curie temperature and dielectric constant for these films.

1. Introduction

Because of the potential applications in various fields of sensor technology and micro-electronic devices, ferroelectric thin films with perovskite structure have attracted great attention. Among these materials, lead titanate (PT) is typical of the perovskite-type ferroelectrics under investigation. The structure and dielectric properties of PT thin films have been well investigated with different techniques, such as x-ray diffraction, scanning electron microscopy, and electrical measurements. However, the lattice dynamics behaviours related to the ferroelectricity in PT thin films have not been completely understood. Recently, several research groups carried out Raman scattering studies to characterize the PT thin films and showed that all transverse optical (TO) phonons tended to depart from the corresponding positions for the bulk single crystal, implying that differences might exist between thin films and bulk single crystals [1–4]. To our knowledge, there has only been one paper published on the Raman spectroscopy of thin ferroelectric films of this material where the temperature dependence of the phonon modes is discussed [5]. However, the soft A_1(1TO) mode, theoretically expected to directly relate to the ferroelectricity on the basis of mean-field

0953-8984/00/040399+16$30.00

as well as self-consistent phonon model calculations [6–8], has not been observed. Thus, it is interesting to examine the dynamic behaviours of phonons in PT thin films.

In this work, Raman scattering is used to study the phonon features in PT thin films deposited by the sol–gel technique on Pt/Si substrates from room temperature up to a temperature (534 °C) higher than the Curie temperature of bulk single crystal, $T_c = 495$ °C [9]. We analyse the spectra obtained with a classical oscillator model to estimate the parameters for the phonons and discuss their temperature behaviours. We have successfully obtained the parameters for the A_1(1TO) soft mode as well as the E(1TO) soft mode from the spectrum. Our results are compared with the data obtained from the literature on bulk material reported by Burns and Scott [10,11]. In contrast to the case for bulk single crystal, the first-order Raman lines do not disappear at the Curie temperature of bulk PT single crystal, and the damping of the soft modes also do not show divergent behaviours at the phase transition point. Using the Lyddane–Sachs–Teller (LST) relation, the clamped dielectric constants, ε_a and ε_c, for the PT thin films have been determined. This indicates that Raman scattering is a powerful tool for characterizing the dielectric properties of ferroelectric thin films.

2. Experimental procedure

The PT thin films were deposited by a sol–gel technique on the Pt-coated Si(100) substrates using multi-layer dip-coating. The detailed processing was described elsewhere [12]. The dipping speed was about 10 cm min^{-1}. Each layer was first dried at 100 °C for 10 min and subsequently heated at 350 °C for 10 min to pyrolyse the organic compounds. The films consisted of ten layers, with each layer approximately 50 nm thick, and were finally annealed at a temperature of 500 °C. A stoichiometric Pb:Ti ratio was used.

The crystal structure and particle size of the thin films were examined by a Rigaku X-ray diffractometer with Cu Kα radiation. Figure 1 shows that the as-prepared thin films were well crystallized without any unexpected phases. The tetragonal structures were confirmed, where the a- and c-axis lattice constants were 0.391 71 nm and 0.410 53 nm, respectively. The preferential c-axis orientation ratio α is calculated to be 0.25 by defining it as $I(001)/[I(001) + I(100)]$, where $I(001)$ and $I(100)$ are the relative intensities of the (001)

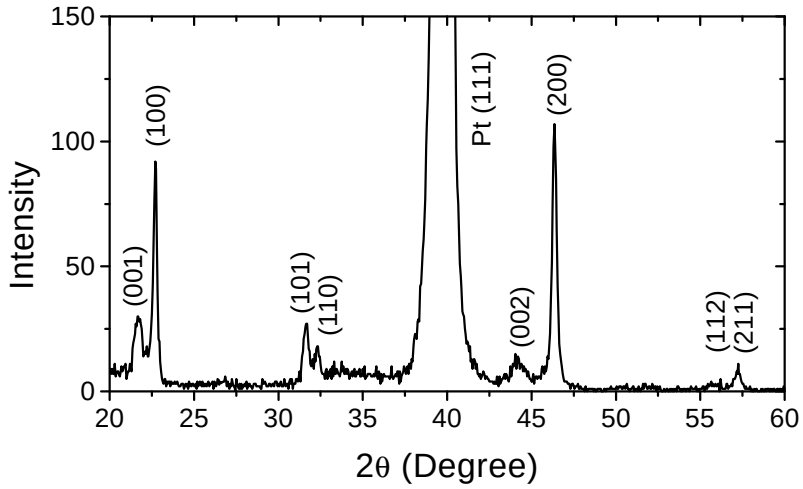

Figure 1. The x-ray diffraction pattern of PT thin film prepared on platinum-coated silicon.

and (100) reflections in the diffraction pattern. The thin films were slightly *a*-axis oriented. The average size of the grains in the films was estimated to be around 47 nm using Scherrer's relationship.

Raman spectroscopy measurements were performed with a Jobin–Yvon RAMANOR HG-2S Raman spectrometer in backscattering geometries. The excitation source was the 488 nm laser radiation from an argon-ion laser and the power of the laser spot on the sample was about 150 mW. The widths of both the entrance and exit slits were set at 300 μm.

The sample was mounted on a metal block located in a temperature-controlled furnace which was constructed from ceramics with a Pyrex window. The temperature of the sample was measured by a thermocouple placed into the metal block near the sample. The variation of the temperature of the sample was less than ± 0.5 °C during the measurements. Since the grains would grow at high temperature, measurement at temperature higher than 534 °C was not carried out. The Raman spectra at room temperature did not change after heating the sample up to 534 °C.

3. Results and discussion

3.1. Mode identification for PT films

In the tetragonal C_{4v}^1 ferroelectric state, there are twelve optic modes in PT which are all Raman active. All modes in the single crystal were observed and identified by Burns and Scott [10, 11], whose labelling system is used throughout the present work. They also showed that the Raman scattering of polycrystalline solids contained all of the essential features of single-crystal Raman spectra even when the crystal spectrum was quite anisotropic [13].

Figure 2 shows the Raman spectrum at room temperature for the PT thin films. In order to identify the mode positions, Raman scattering for a commercial PT powder with an average diameter of 1.2 μm is also shown in figure 2. The corresponding mode frequencies for the PT thin films are listed in table 1. They are identified by comparing each line for the films with those of the powder spectrum in figure 2. It is found that the film spectrum has a reasonable resemblance to that of the powder. However, there are several differences between the thin-film and the powder spectra. The peaks for the thin films are broad and all of the TO modes are shifted to lower frequencies. In addition, an unexpectedly high degree of quasi-elastic

Table 1. Phonon frequencies (cm^{-1}) in $PbTiO_3$ single crystal and thin film.

	Single crystal		Thin film
Phonon mode	$P \sim 0$ GPa[a]	$P \sim 1.35$ GPa[b]	Pt/Si
E(1TO)	89	80	80
A_1(1TO)	127	117	118
E(2TO)	221	201	209
B_1 + E	290	287	289
A_1(2TO)	364	336	334
E(2LO) + A_1(2LO)	445	—	443
E(3TO)	508	504	504
A_1(3TO)	651	607	604
E(3LO)	717	—	728
A_1(3LO)	797	746	—

[a] Reference [10].
[b] Reference [20].

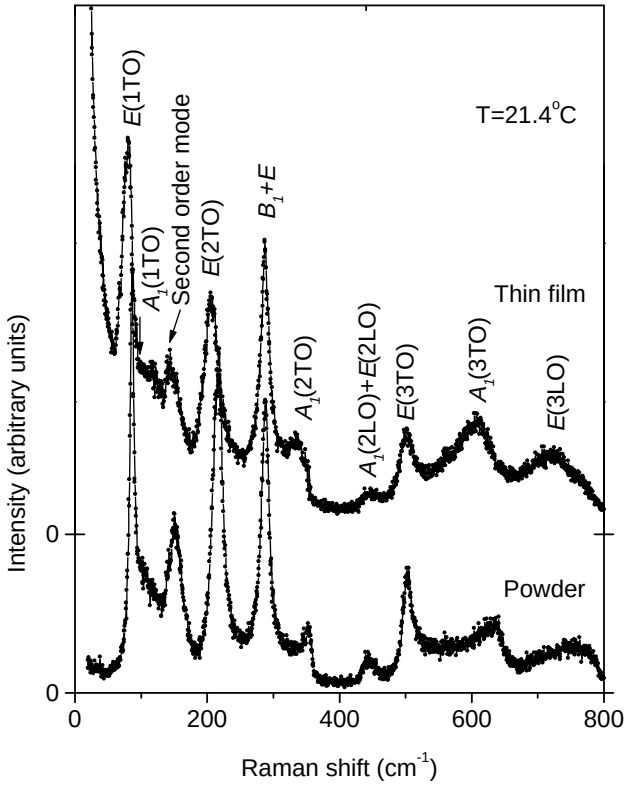

Figure 2. Raman spectra at room temperature for PT thin film prepared on platinum-coated silicon and PT powder.

scattering occurred near the Rayleigh line in the low-frequency region of the film spectrum, indicating that an unknown structure might exist in the thin films. Recent Raman scattering investigation for bulk PT single crystal shows that a relaxation mode associated with a central peak appears below the soft-phonon line when the cubic–tetragonal phase transition is approached [14]. It seems that the intense quasi-elastic scattering in the thin films can be attributed to the relaxation process which describes the order–disorder mechanism. However, it is not clear at present why low-dimensional systems such as thin films as well as ultra-fine particles [15] show such significant central-mode behaviour at temperatures far from the phase transition.

3.2. Soft-mode frequencies

Figure 3 shows some of the typical (10–110 cm^{-1}) Raman spectra of the soft-phonon modes at several temperatures. It is surprising that the Raman scattering does not disappear on heating through the transition temperature of bulk PT single crystal (493 °C). The intense Raman scattering remains up to a temperature as high as 534 °C. In view of the fact that the growth of PT grains due to the high temperature would very likely influence the film properties, further heating experiments were not carried out. It was also found that the Raman scattering intensity increases rapidly with temperature up to about 479 °C, and then decreases. This feature is quite different from the situation occurring in the PT bulk and ultra-fine-particle materials. Note that

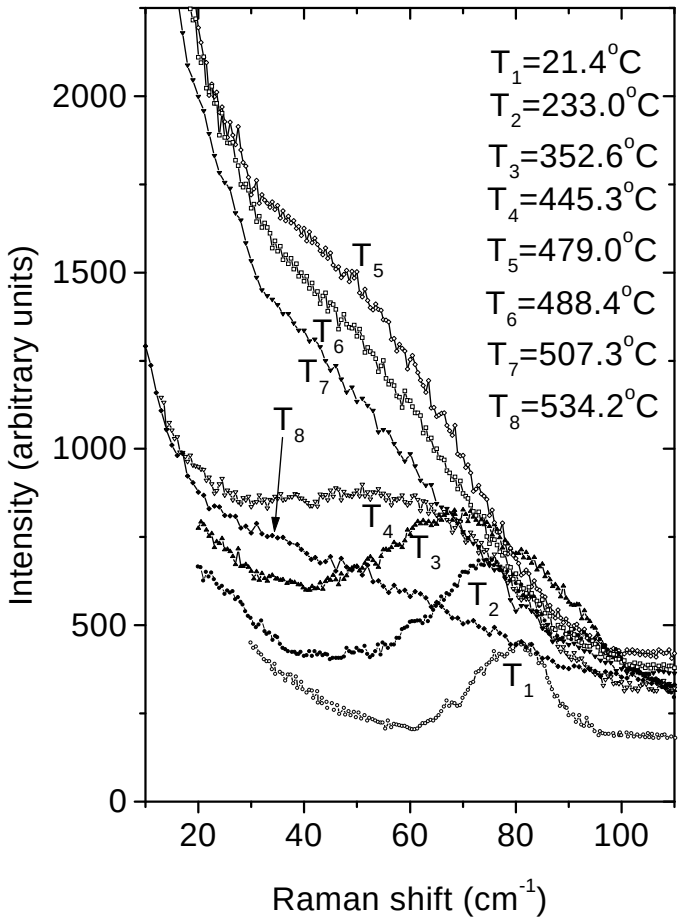

Figure 3. Raman spectra of the soft phonons for PT thin film at various temperatures.

the A_1(1TO) mode is fairly weak at room temperature, but its existence can be verified from the temperature dependence of the spectra as shown in figure 4. Since the mode linewidth is quite broad and the E(1TO) and A_1(1TO) modes overlap, their peak positions cannot be resolved easily.

Here the usual model of the damped classical harmonic oscillator has been used to estimate the parameters for the modes [10, 11, 16]. On the assumption that the quasi-elastic scattering has a line shape of Lorentz type, the Raman line containing quasi-elastic scattering, and soft E(1TO) and A_1(1TO) modes can be expressed as [16]

$$I(\omega) = \frac{h}{4\omega^2 + w_q^2} + \sum_{i=1}^{2} \frac{F_i \Gamma_i \omega_{0i}^3}{(\omega_{0i}^2 - \omega^2)^2 + 4\Gamma_i^2 \omega_{0i}^2 \omega^2} \tag{1}$$

where w_q is the full width at half-maximum (FWHM) for the quasi-elastic scattering, h is a constant, $i = 1$ and 2 correspond to the E(1TO) and A_1(1TO) modes, respectively, and F_i, ω_{0i}, and Γ_i are the scale factor, mode frequency, and damping factor of the two phonons. Equation (1) is employed to calculate the parameters for the soft modes by a computer-fitting procedure. Here, we have made a non-linear least-squares fit based on the Levenberg–Marquardt method [17], using Origin (Version 5) software developed by Microcal Software.

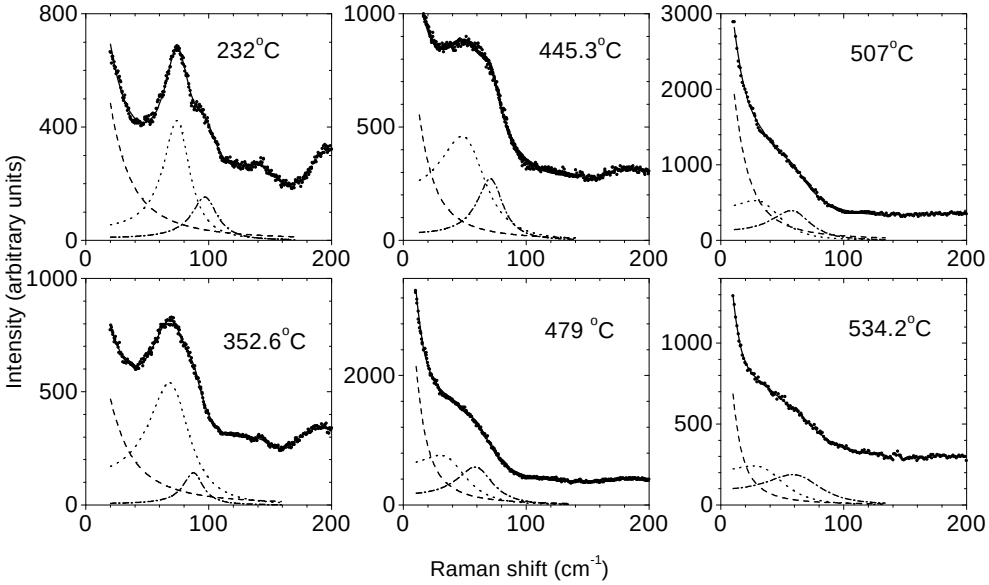

Figure 4. Typical spectra of the soft phonons for PT thin film as functions of temperature. The full lines represent the fitting results. The dashed (- - - -), dotted (· · · · · ·), and chain (— · —) lines are the best-fit profiles of the quasi-elastic scattering, the E(1TO), and the A_1(1TO) soft modes.

The fits are quite satisfactory when a frequency-independent damping constant for each of the soft modes is used as in the case of bulk PT single crystal. Figure 4 shows the results of the fitting using equation (1) in such a way that the quasi-elastic scattering and the two soft modes are seen separately. It should be noted that although the fits were repeated to give the best results, changing the initial values of the mode parameters, the uncertainties in the damping constants and frequencies obtained, given by the error bars in figure 5 and figure 6, are still quite large, particularly at high temperatures. This is presumably due to the fact that the soft modes became overdamped, and overlapped with the broad quasi-elastic scattering at high temperatures. As shown in figure 4, the intensity of the A_1(1TO) soft modes become stronger and stronger with respect to that of the E(1TO) soft modes with increasing temperature.

The temperature dependence of the E(1TO) and A_1(1TO) soft-mode frequencies in PT thin films is shown in figure 5. The behaviour of PT thin films is compared, in the figure, with the results obtained from Raman scattering for bulk PT single crystal [10]. The behaviour of PT thin films substantially differs from that of bulk PT single crystal in the following respects.

(a) There is a clear downward shift in the frequencies of the soft modes in the PT films below the Curie temperature of bulk PT single crystal.
(b) The soft modes are still present above the Curie temperature of bulk PT single crystal, in contrast to the cases for bulk [10] and ultra-fine-particle materials [15].

It seems there is a transition point around 479 °C above which the modes show a hardening trend rather than a softening, in particular for the A_1(1TO) mode. The present result for the E(1TO) soft mode is in agreement with that reported by Taguchi *et al* [5], which is also shown in figure 5, except for the high-temperature region. However, they have not measured the temperature dependence of the A_1(1TO) mode, and have not observed the hardening behaviours of the soft modes above the Curie temperature of bulk PT single crystal.

On the basis of the fact that dielectric constant would diverge upon heating at a temperature

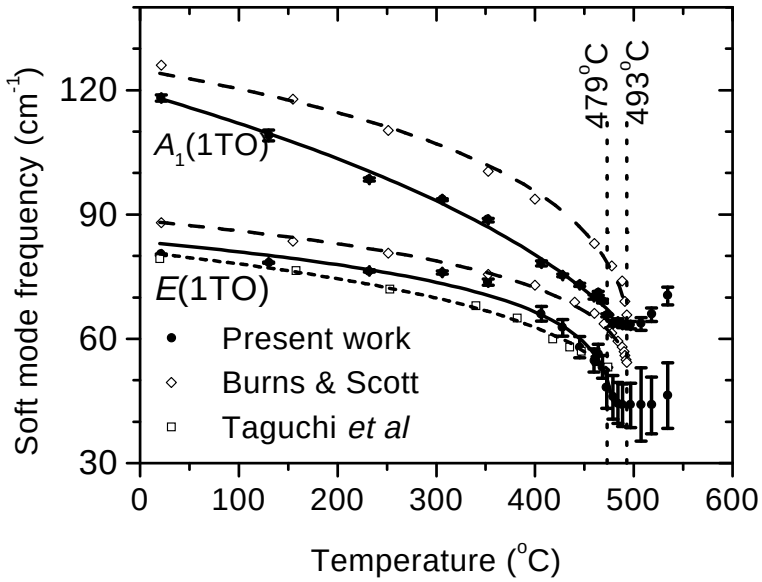

Figure 5. The temperature dependence of the E(1TO) and A_1(1TO) soft phonons for PT thin film (●). The open diamonds (◊) and squares (□) show the results for single crystal taken from reference [10] and for thin film from reference [5], respectively. The lines are calculated using equation (2).

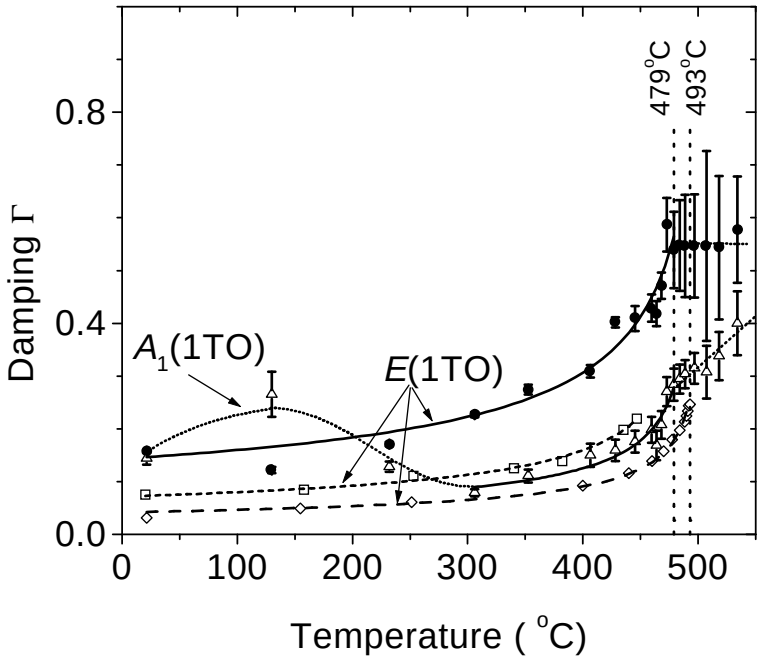

Figure 6. The damping factor as a function of temperature for the A_1(1TO) (△) and E(1TO) (●) soft phonons in PT thin films. The open diamonds (◊) and squares (□) represent the results for the E(1TO) mode for single crystal [10] and for thin film [5], respectively. The full (——), dashed (- - - -), and broken (– – –) lines are calculated using equation (2). The other curves are to guide the eye.

T_u, above T_c, Burns and Scott proposed the following empirical relationship for analysing the temperature dependence of soft-mode frequencies [10]:

$$\omega(T) = G(T_u - T)^n \tag{2}$$

where

$$T_u = T_0 + \frac{4}{3}(T_c - T_0) \tag{3}$$

where T_0, T_c, n, and G are the Curie–Weiss temperature, the Curie temperature, and constants, respectively. We have used this relationship to fit all the data presented in figure 5. Since both theoretical calculation and experiments indicate that the T_cs of low-dimensional systems are not identical to that of bulk material [15, 18, 19], and the exact values of T_c and T_0 for PT thin films are not known yet, we cannot calculate T_u by using equation (3), so we must regard it as a fitting parameter. The fitted curves are shown in figure 5. It can be seen that the fits are very good in the temperature range given in table 2. The parameters obtained are also listed in table 2. It is worth emphasizing that $T_u = 577\ ^\circ$C derived for the A_1(1TO) mode in the PT thin films is identical with that obtained from the temperature dependence of the *c*-axis dielectric constant (this will be discussed in section 3.5). This indicates that the ferroelectric phase should persist for temperature up to 577 °C for these PT films.

Table 2. Parameters of the empirical fits to the A_1(1TO) and E(1TO) frequencies and their damping factors in $PbTiO_3$.

		Thin films			Single crystal	
		Present work		Taguchi *et al*[a]	Burns and Scott[b]	
		E(1TO)	A_1(1TO)	E(1TO)	E(1TO)	A_1(1TO)
ω	G (cm^{-1})	37.6	14.1	28.2	39.4	42.8
	n	0.129	0.336	0.169	0.130	0.172
	T_u (°C)	483	577	514	507	507
	T-range (°C)	21.4–479	21.4–479	20–474	23–493	23–493
Γ	G (cm^{-1})	3.244	1.245	1.604	0.938	—
	n	$-\frac{1}{2}$	$-\frac{1}{2}$	$-\frac{1}{2}$	$-\frac{1}{2}$	—
	T_u (°C)	512	499	501	507	—
	T-range (°C)	21.4–479	306–479	20–447	23–493	—

[a] Reference [5].
[b] Reference [10].

3.3. Soft-mode damping

Figure 6 shows the damping factor Γ obtained via equation (1) for the E(1TO) and A_1(1TO) soft modes. For comparison, we recalculate the Burns and Scott [11] data via

$$\Gamma = \frac{\gamma}{2\omega_0} \tag{4}$$

where they used γ to describe the damping of E(1TO) in bulk PT single crystal. The calculated data are also plotted in figure 6 as the broken line. Here, the damping factor Γ for PT thin film is found not to diverge, in contrast to that for the bulk PT single crystal [10, 11]. The damping factor of the E(1TO) mode increases as the temperature increases, reaches a maximum around 479 °C, and then remains constant. The damping factor is larger for PT thin films than for PT bulk single crystal. The Raman linewidth of natural PT is related to the lifetime of the phonon

created in the Raman process. The primary broadening mechanism for perfect crystal is the decay of the optical phonon into two acoustic phonons with opposite wave vectors. Thus the large damping indicates that the phonon lifetime in the thin films is less than in the bulk single crystal.

As can be seen in figure 6, the A_1(1TO) mode shows more complicated behaviour and the damping factor does not increase monotonically like the E(1TO) mode below 479 °C. Above this temperature, it tends to increase slowly like the variation of its mode frequency. To our knowledge, the temperature dependence of the damping factor of the A_1(1TO) soft mode has not been experimentally observed for bulk single crystals. This is related to the fact that the A_1(1TO) soft mode is not observable at atmospheric pressure [20, 21]. However, several research groups have reported that the A_1(1TO) soft mode obviously exists in PT thin films [2–4, 22]. Thus, PT thin films provide a good basis for the study of damping behaviour of the A_1(1TO) soft mode.

We also tried to fit the temperature dependence of Γ via the empirical form of equation (2). Note that the damping factors show complicated behaviours in the present case, so it is impossible to fit the data in the same form over the whole temperature range. The results with the temperature intervals used for fitting are listed in table 2. Figure 6 indicates that an agreement with the experimental points is obtained with $n = -\frac{1}{2}$ for all cases in the corresponding temperature intervals. There is a slight difference from the result obtained by Burns and Scott [10], in which the damping was described as γ and $n \neq -\frac{1}{2}$.

Several models have been proposed for the temperature dependence of the damping constant [23–25]. On the basis of a one-dimensional model, a singular behaviour for the damping has been predicted [24]. But for a three-dimensional system, it is shown that the soft-mode damping is finite at the transition temperature [25]. The present work on PT thin films seems to support the latter viewpoint.

3.4. High-frequency modes

In this section we discuss the results for the high-frequency modes, i.e. all of the modes excluding the E(1TO) and A_1(1TO) modes. Figure 7 shows typical Raman spectra for high-frequency modes (100–800 cm^{-1}) at several temperatures. Note that all observed modes at higher temperature have the same features as at low temperature, and are inherently different from the second-order broad structures observed in the cubic phase of $BaTiO_3$ above T_c [26,27]. Thus, the fact that the Raman intensity is still observed and modes do not disappear at T_c for bulk PT single crystal is made clear again.

Figure 8 gives the phonon frequencies as a function of temperature. As can be seen, our data are generally in agreement with the results of Taguchi *et al* [5] in the low-temperature range. The temperature dependence of modes in PT thin films is similar to the case for bulk single crystal. However, some facts are worthy of note. First, the TO mode frequencies are generally lower than those of the corresponding modes in bulk single crystal. Second, above 400 °C, the variation of the TO modes with temperature appears to have a slow trend.

3.5. Dielectric behaviour

Characterization of the dielectric constants of thin films is of considerable importance from both practical and fundamental viewpoints. The Raman scattering technique provides a possible approach to estimating the intrinsic dielectric constants along the principal axes of crystal in the films, which might be very difficult to obtain by electrical measurements at the present state of the art. If all of the phonon modes are determined, the dielectric constant can be calculated

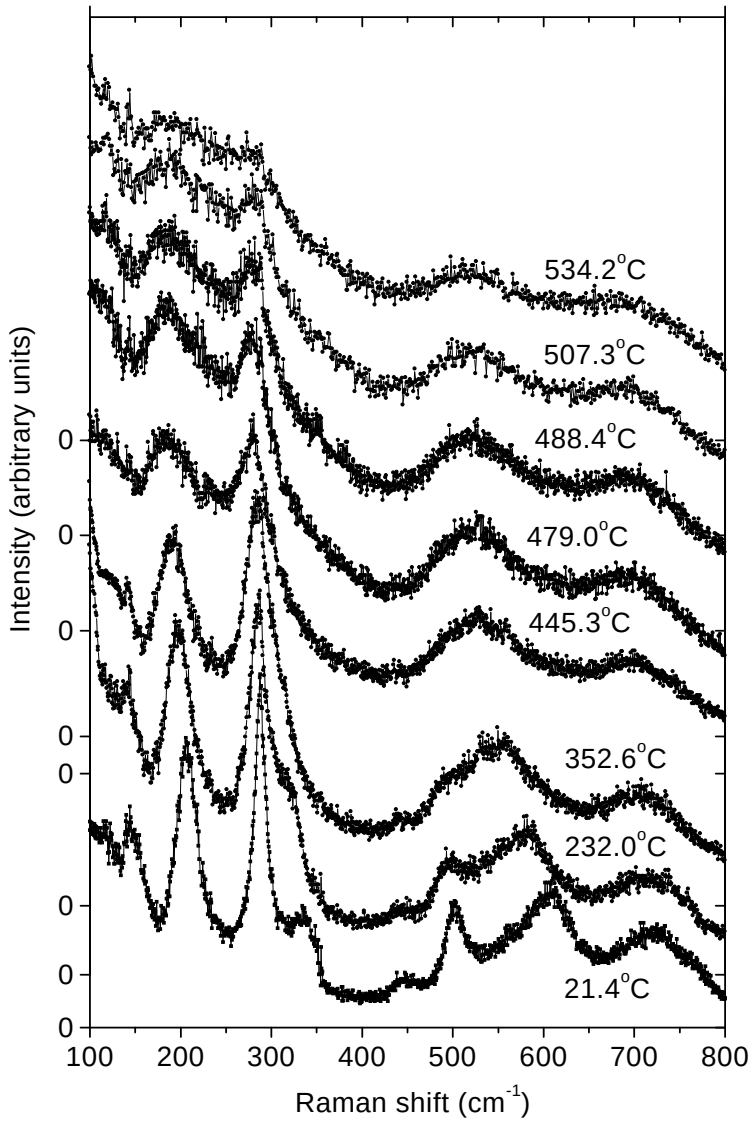

Figure 7. Typical Raman spectra of the high-frequency modes for PT thin film at various temperatures.

in a straightforward manner using the Lyddane–Sachs–Teller (LST) relationship:

$$\frac{\varepsilon(0)}{\varepsilon_\infty} = \frac{\omega_{1\mathrm{LO}}^2}{\omega_{1\mathrm{TO}}^2}\frac{\omega_{2\mathrm{LO}}^2}{\omega_{2\mathrm{TO}}^2}\frac{\omega_{3\mathrm{LO}}^2}{\omega_{3\mathrm{TO}}^2} \tag{5}$$

where $\varepsilon(0)$ is the clamped dielectric constant at zero frequency and ε_∞ is the optical dielectric constant. In the ferroelectric phase, the dielectric constant along the ferroelectric c-axis, $\varepsilon_c(0)$, is determined by the frequencies of the A_1 modes, and the dielectric constant perpendicular to the c-axis, $\varepsilon_a(0)$, is determined by the frequencies of the E modes. As shown in figure 5 and figure 8, all phonon modes, except the E(1LO) and A_1(1LO) modes, have been measured. However, accounting for that:

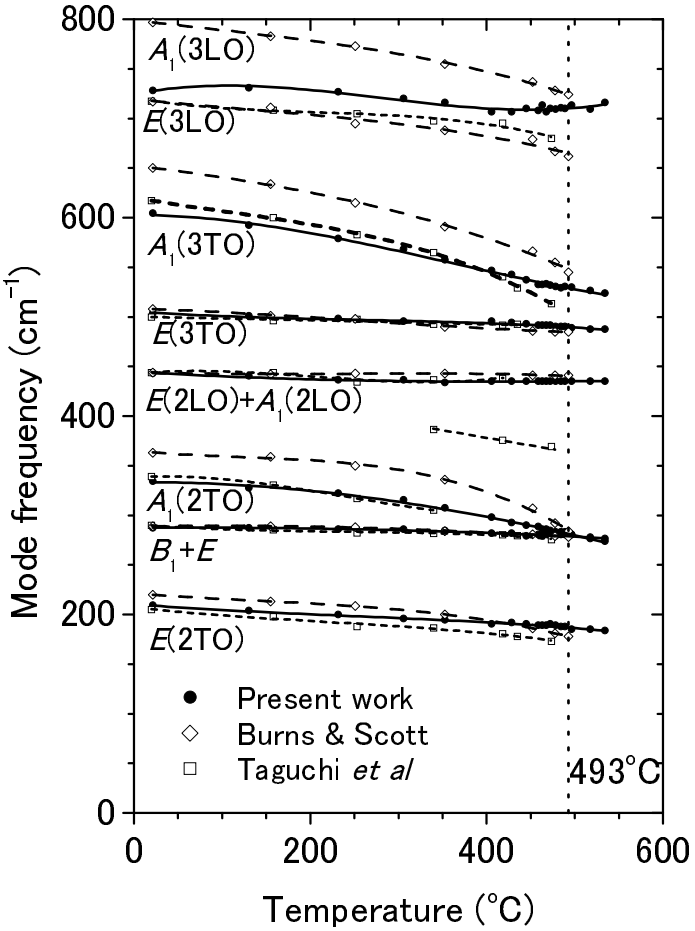

Figure 8. The temperature dependence of the high-frequency modes in PT. The full (——), dashed (- - - -), and broken (– – –) lines represent least-squares fits to thin-film data from the present work (●) and Taguchi *et al* [5] (□), and single-crystal data taken from reference [10] (◇), respectively, using polynomials with up to cubic terms in T.

(a) the soft modes dominate the dielectric constants in the ferroelectric phase [10];
(b) the LO modes appear not to depart from their positions in bulk single crystal;
(c) the LO modes vary less with temperature than do the TO modes [10];

the values of unobserved LO modes are taken as those of the bulk at room temperature [10] in the calculation of the dielectric constant from equation (5). Taking [28] $\varepsilon_\infty = (2.66)^2 = 7.08$, we obtain $\varepsilon_a(0) = 164$ and $\varepsilon_c(0) = 71$. Due to the absence of directly measured data, the evaluation of $\varepsilon_a(0)$ is not confirmed. However, the estimate of $\varepsilon_c(0)$ is in excellent agreement with the results for highly *c*-axis-oriented PT thin films deposited on MgO single crystal, which give a value of 70 on extrapolating the orientation dependence of the dielectric constant [29]. Thus, the LST relationship can be applied for PT thin films as well as for bulk PT single crystal, in contrast to the case for $BaTiO_3$ [30].

The temperature dependence of $\varepsilon_a(0)$ and $\varepsilon_c(0)$ determined via equation (5) is shown in figure 9. It should be noted that the maximum around 493 °C is not corresponding to a transition from a tetragonal to a cubic phase on the basis of the Raman selection rules.

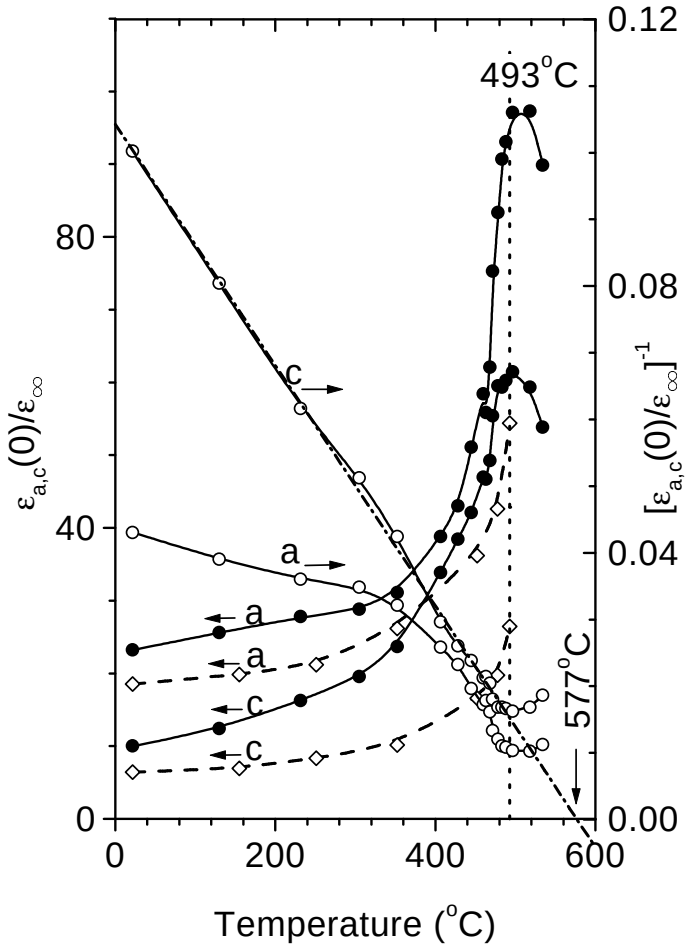

Figure 9. The temperature dependence of the dielectric constants (●) and their inverse (○) for PT thin film along the *a*- and *c*-axes calculated from the LST relation. The slope of the chain line (— · —) is used to evaluate the Curie–Weiss constant. The open diamonds (◇) represent the results for bulk PT single crystal [10]. The other lines are used to guide the eye.

Devonshire phenomenological theory predicts a Curie–Weiss law for the dielectric constant along the ferroelectric axis (*c*-axis). For first-order phase transition, $\varepsilon_c(0)$ in the ferroelectric phase is expressed as

$$\frac{\varepsilon_\infty}{\varepsilon_c(0)} = \frac{8\varepsilon_\infty(T_u - T)}{C^\star} \tag{6}$$

where $C^\star$ is the Curie–Weiss constant. It is clear from figure 9 that $\varepsilon_c(0)$ obeys the Curie–Weiss law very well over a wide temperature interval. The Curie–Weiss constant for PT thin films, $C^\star_{\text{film}}$, is evaluated to be 3.27×10^5 °C from figure 9. This result agrees with those reported for the bulk single crystal by Samara [31] and Remeika and Glass [9], who showed $C^\star_{\text{bulk}} = 4.4 \times 10^5$ °C and 4.1×10^5 °C, respectively. This may be regarded as support for the correct assignment to A_1(1TO) in PT thin films. The mode frequencies and symmetry assignments given by Burns and Scott [10] were questioned recently by some authors on the basis of consideration of the polarization and angular dependence of the phonon modes [14,32].

However, the present case shows that Burns and Scott's assignment is correct. $T_u = 577\ ^\circ C$ determined here is identical to that derived from the temperature dependence of the $A_1(1TO)$ mode frequency by an empirical fit as described in section 3.2. This confirms to us once again that the ferroelectric phase can exist up to as high as 577 °C for these films.

3.6. The stress effect

As described above, Raman scattering measurements for the PT thin films deposited on Pt/Si substrates show that:

(a) the cubic–tetragonal phase transition occurs at a temperature more than 40 °C higher than that expected for bulk PT single crystals;
(b) the dielectric constant along the principal axis is remarkably larger than that of bulk PT single crystal;
(c) the soft modes obviously shift towards low frequencies.

From the mean-field as well as the self-consistent phonon model calculations, the frequencies of the $A_1(1TO)$ soft mode are expected to be proportional to the spontaneous polarization P_s in the ferroelectric phase [6–8]. Thus, the lowering of the $A_1(1TO)$ mode frequency means that P_s for PT thin film is less than that for bulk PT single crystal. These results are supported by other measurements on the perovskite-structure thin films epitaxially grown on single-crystal substrates [29,33]. The Curie temperature was observed to shift upwards to 515 °C–535 °C by means of high-temperature x-ray diffraction, and the electrical measurement gave an estimate of the dielectric constant for the perfectly *c*-oriented PT thin film as having a value of 70 [29]. For a 30-layer $BaTiO_3$ ultra-thin film deposited on $SrTiO_3$ single crystal, it was found that the phase transition of the film took place at temperatures up to 600 °C while the P_s was smaller than that for the bulk crystal [33]. In this section, we propose a possible explanation for the observed phenomena within the framework of Devonshire theory [34].

Two mechanisms are possible for inducing the downshift of the TO mode frequencies in PT materials. The first is the downshift induced by the particle-size effect. Recent work on Raman scattering measurements for PT ultra-fine particles shows that the TO modes shift toward low frequency with decrease of particle size [15]. However, the Raman shift in the particles larger than 52 nm shows no difference from that in the bulk single crystal. The particle size in the present films was determined to be 47 nm using x-ray diffraction. It seems that the obvious downshift of the TO mode frequencies is not attributable to a particle-size-induced effect. The second mechanism is that the observed displacement arises from the stress effect [20]. As shown in table 1, the phenomenon of the frequency shifts at room temperature looks like the hydrostatic pressure effect on bulk PT single crystal, indicating that the film is subjected to a high stress around 1.35 GPa. However, the residual stress in the PT thin films appears to be anisotropic, since the hydrostatic pressure will lead to a decrease of the Curie temperature at high pressure [31]. Recently, it has been suggested that a two-dimensional stress model based on Devonshire theory can be very effective in explaining the shift of the Curie point in epitaxial PT thin films [35,36]. But it predicts that the dielectric constant along the *c*-axis at room temperature will decrease under the same stress condition, in contrast to the present results. It is necessary to modify the model to explain the related phenomena.

We express the free energy of ferroelectric materials as a function of polarization and stress as proposed by Devonshire. Under the assumption that the stress component perpendicular to the surface of the film is relaxed and thus only a biaxial stress acts in the plane of the film, the appropriate free-energy function for PT is

$$F = F_0 + \frac{1}{2}\alpha_0(T - T_0)P^2 - \frac{1}{4}BP^4 + \frac{1}{6}CP^6 - D\sigma^2 - \frac{1}{2}\alpha\sigma P^2 - \frac{1}{4}\beta\sigma P^4 \qquad (7)$$

where P is the polarization perpendicular to the film surface, T the temperature, T_0 the Curie–Weiss temperature, σ the in-plane biaxial stress, $\alpha_0 = 1/C^\star$, B, C, D, α, β constants, and F_0 the free energy of the unpolarized state without stress.

The spontaneous polarization is determined by the stability condition

$$\frac{\partial F}{\partial P} = 0 \tag{8}$$

or

$$P_s^2 = \frac{1}{2C}\left[(B+\beta\sigma) + \sqrt{\frac{1}{4}(B+\beta\sigma)^2 - 4\alpha_0 C(T-T_c)}\right]. \tag{9}$$

Here T_c is the Curie temperature:

$$T_c = T_0 + \frac{3(B+\beta\sigma)^2}{16\alpha_0 C} + \frac{\alpha\sigma}{\alpha_0}. \tag{10}$$

It can be derived from equation (8) and the following condition:

$$F(P_c) = F(P=0) \tag{11}$$

at $T = T_c$, where P_c is the polarization at the Curie temperature. The appropriate second partial derivative of equation (7) gives the reciprocal dielectric constant along the polarization axis:

$$\varepsilon^{-1} = \alpha_0(T-T_0) - \alpha\sigma - 3(B+\beta\sigma)P_s^2 + 5CP_s^4. \tag{12}$$

In the vicinity of T_c, P_s^2 can be expanded as

$$P_s^2 = \frac{1}{2C}\left[\frac{3}{2}(B+\beta\sigma) - \frac{4\alpha_0 C(T-T_c)}{B+\beta\sigma}\right]. \tag{13}$$

Substituting equation (13) into (12), we have

$$\varepsilon^{-1} = -8\alpha_0(T-T_c) + \frac{3}{4C}(B+\beta\sigma)^2. \tag{14}$$

Using equation (10) and (14), we can discuss the influence of stress on the shift of the Curie temperature and dielectric constant for PT thin films. From these two equations, the stress dependences of T_c and ε^{-1} are obtained:

$$\frac{\partial T_c}{\partial\sigma} = \frac{1}{\alpha_0}\left(\alpha + \frac{1}{2}\beta P_c^2\right) \tag{15}$$

and

$$\frac{\partial\varepsilon^{-1}}{\partial\sigma} = 8\alpha + 6\beta P_c^2. \tag{16}$$

If we take $\beta = 0$, equations (15) and (16) will give the same results as those predicted by Rossetti *et al* [35] and Yamamoto and Matsuoka [36]. For a two-dimensional compressive stress, $\sigma < 0$, $\alpha < 0$; thus $\Delta T_c > 0$ and $\Delta\varepsilon^{-1} > 0$ (Δ denotes the deviation from the non-stressed state). However, experimental results show that although the Curie temperature shifts upward, the dielectric constant along the polarization axis increases; that is, $\Delta\varepsilon^{-1} < 0$. Thus, β cannot be regarded as zero; in other words, the high-order term $\beta\sigma P^4$ must be included in the expansion of the free-energy function. Here, we estimate the magnitude of β. Since $\Delta T_c > 0$ and $\Delta\varepsilon^{-1} < 0$, using equations (15) and (16), the following inequality is obtained:

$$-\frac{4}{3}\frac{\alpha}{P_c^2} < \beta < -\frac{2\alpha}{P_c^2}. \tag{17}$$

We conclude that the shifts in the Curie temperature and in the dielectric constant along the polarization axis can be plausibly explained by a modified Devonshire theory based on two-dimensional compressive stress.

4. Conclusions

The dynamic behaviours for PT thin films grown by the sol–gel technique on Pt/Si have been studied with Raman scattering. A central-mode-type scattering is found to be always present in the samples, and becomes more and more intensive on heating toward the phase transition. The two soft modes, E(1TO) and A_1(1TO), are separated successfully from the Raman spectrum, and do not soften further near the phase transition. The damping of the soft modes is larger in the thin film than in the bulk single crystal, and does not show a divergent behaviour on approaching the phase transition. The temperature dependence of the dielectric constant along the principal axis is evaluated using the LST relationship, showing that Raman scattering provides a promising approach for analysing the dielectric properties of thin film or microcrystal. A shift of the phase transition temperature is found, and this might be explained by the Devonshire theory. It is clear that the thin film shows some different features from bulk crystals. Further studies of the ferroelectricity of PT thin films are thus needed.

Acknowledgments

The authors thank Professor M Minakata for helpful discussion. One of the authors (DSF) is grateful to the Japanese Government for providing the scholarship that enabled him to carry out this work. Part of this work was supported by a Grant-in-Aid for General Scientific Research (B) from the Ministry of Education, Science, and Culture of Japan (No 09450126).

References

[1] Ma W, Zhang M, Yu T, Chen Y and Ming N 1998 *Appl. Phys.* A **66** 345
[2] Sun L, Chen Y F, He L, Ge C Z, Ding D S, Yu T, Zhang M S and Ming N B 1997 *Phys. Rev.* B **55** 12 218
[3] Feng Z C, Kwaqk B S, Erbil A and Boatner L A 1993 *Appl. Phys. Lett.* **62** 349
[4] Ching-Prado E, Reynés-Figueroa A and Katiyar R S 1995 *J. Appl. Phys.* **78** 1920
[5] Taguchi I, Pignolet A, Wang L, Proctor M, Lévy F and Schmid P E 1993 *J. Appl. Phys.* **73** 394
[6] Feder J and Pytte E 1970 *Phys. Rev.* B **1** 4803
[7] Gills N S and Koehler T R 1972 *Phys. Rev.* B **5** 1925
[8] Pytte E 1972 *Phys. Rev.* B **5** 3758
[9] Remeika J P and Glass A M 1970 *Mater. Res. Bull.* **5** 37
[10] Burns G and Scott B A 1973 *Phys. Rev.* B **7** 3088
[11] Burns G and Scott B A 1970 *Phys. Rev. Lett.* **25** 167
[12] Suzuki H, Othman M B, Murakami K, Kaneko S and Hayashi T 1996 *Japan. J. Appl. Phys.* **35** 4896
[13] Burns G and Scott B A 1970 *Phys. Rev. Lett.* **25** 1191
[14] Fontana M D, Idrissi H, Kugel G E and Wojicik K 1991 *J. Phys.: Condens. Matter* **3** 8695
[15] Ishikawa K, Yoshikawa K and Okada N 1988 *Phys. Rev.* B **37** 5852
[16] DiDomenico M Jr, Wemple S H and Porto S P 1968 *Phys. Rev.* **174** 522
[17] Press W *et al* 1988 *Numerical Recipes in C. The Art of Scientific Computing* (New York: Cambridge University Press)
[18] Zhong W L, Wang Y G, Zhang P L and Qu B D 1994 *Phys. Rev.* B **50** 698
[19] Li S, Eastman J A, Vetrone J M, Foster C M, Newnham R E and Cross L E 1997 *Japan. J. Appl. Phys.* **36** 5169
[20] Sanjurjo J A, López-Cruz E and Burns G 1983 *Phys. Rev.* B **28** 7260
[21] Cerderia F, Holzapfel W B and Bäuerle D 1975 *Phys. Rev.* B **11** 1188
[22] Ma W H, Zhang M S and Yin Z 1998 *J. Korean Phys. Soc.* **32** S1137
[23] Silverman B D 1972 *Solid State Commun.* **10** 311
[24] Tani K 1969 *J. Phys. Soc. Japan* **26** 93
[25] Pytte E 1970 *Phys. Rev.* B **1** 924
[26] Fontana M P and Lambert M 1972 *Solid State Commun.* **10** 1
[27] Burns G and Dacol F H 1978 *Phys. Rev.* B **18** 5750
[28] Pastrnak J and Cross L E 1971 *Phys. Status Solidi* b **44** 313
[29] Iijima K, Tomida Y, Takayama R and Ueda I 1986 *J. Appl. Phys.* **60** 361

[30] Li Z, Chan S K, Grimsditch M H and Zouboulis E S 1970 *J. Appl. Phys.* **70** 7327
[31] Samara G A 1971 *Ferroelectrics* **2** 277
[32] Foster C M, Li Z, Grimsditch M, Chan S K and Lam D J 1993 *Phys. Rev.* B **48** 10 160
[33] Yoneda Y, Okabe T, Sakaue K and Terauchi H 1998 *J. Appl. Phys.* **83** 2458
[34] Devonshire A F 1949 *Phil. Mag.* **40** 1040
[35] Rossetti G A Jr, Cross L E and Kushida K 1991 *App. Phys. Lett.* **59** 2524
[36] Yamamoto T and Matsuoka H 1994 *Japan. J. Appl. Phys.* **33** 5317